Available online at www.sciencedirect.com
SCIENCE DIRECT®
Journal of Organometallic Chemistry 689 (2004) 1370–1376
Journal of Organometallic Chemistry
www.elsevier.com/locate/jorganchem

Synthesis and properties of oligomers of iron–manganese carbonyl complexes with bridging disulfido ligands

Richard D. Adams *, Burjor Captain, O-Sung Kwon, Perry J. Pellechia, Sanghamitra Sanyal

Department of Chemistry and Biochemistry, University of South Carolina, Columbia, SC 29208, USA

Received 16 September 2003; accepted 17 December 2003

Abstract

The reactions of activated $CpFeMn(CO)_7$ **1a** and $Cp^*FeMn(CO)_7$ **1b**, $Cp = C_5Me_5$ with thiirane yielded the new dimeric mixed metal disulfido complexes: $[CpFeMn(CO)_5(\mu_3\text{-}S_2)]_2$ (**2**) and $[Cp^*FeMn(CO)_5(\mu_3\text{-}S_2)]_2$ (**3**). Compounds **2** and **3** both contain two triply bridging disulfido ligands. When heated at 40 °C, compound **2** was transformed into a trimeric compound $Cp_3Fe_3Mn_3(CO)_{15}(\mu_3\text{-}S_2)(\mu_4\text{-}S_2)_2$, **4**. Compound **4** contains three disulfido ligands, each of which has a different bridging coordination mode in the six atom metal cluster. There are three inequivalent $CpFe(CO)_2$ groupings linked to a central $Mn_3(S_2)_3$ core by the disulfido ligands. In solution, compound **4** exhibits a dynamical intramolecular exchange process that interconverts two of the three $CpFe(CO)_2$ groups on the NMR timescale.

Keywords: Disulfido ligands; Iron; Manganese; Oligomers; Molecular dynamics

1. Introduction

The syntheses of metal cluster complexes are facilitated by using bridging ligands derived from the main group elements [1]. The sulfido ligand has been shown to be one of the most effective ligands for the synthesis and stabilization of higher nuclearity metal cluster complexes because of its ability to bond simultaneously to several metal atoms [2]. The disulfido ligand can also exhibit a variety of bridging coordination geometries in polynuclear metal complexes [3], and it is also useful in facilitating the aggregation of metal atoms into higher nuclearity metal complexes [4]. Transition metal complexes containing the disulfido ligand also exhibit a range of interesting reactivity toward organic molecules involving insertions into the sulfur–sulfur bond [5].

Recently, we have reported the new disulfido manganese containing complexes, $Mn_2(CO)_7(\mu\text{-}S_2)$ [6,7] and $CpMoMn(CO)_5(\mu\text{-}S_2)$ [8] that have been found to be good reagents for the synthesis of a wide range of new sulfido metal carbonyl complexes by insertions into the sulfur–sulfur bond [9]. $Mn_2(CO)_7(\mu\text{-}S_2)$ is conveniently prepared by the reaction of $Mn_2(CO)_9(NCMe)$ with thiirane [6,7].

In an effort to prepare a heterodinuclear iron–manganese homologue of $CpMoMn(CO)_5(\mu\text{-}S_2)$, we have investigated the reactions of $CpFeMn(CO)_7$ **1a** and $Cp^*FeMn(CO)_7$ **1b**, $Cp = C_5Me_5$ activated by Me_3NO with thiirane. Instead of obtaining the heterodinuclear product, dimers $[CpFeMn(CO)_5(\mu_3\text{-}S_2)]_2$ (**2**) and $[Cp^*FeMn(CO)_5(\mu_3\text{-}S_2)]_2$ (**3**) were obtained. Furthermore, when heated, compound **2** was converted into a trimer $Cp_3Fe_3Mn_3(CO)_{15}(\mu_3\text{-}S_2)(\mu_4\text{-}S_2)_2$, **4** that exhibits interesting molecular dynamics on the NMR timescale in solution. The results of these studies are reported here.

* Corresponding author. Tel.: +1-803-777-7187; fax: +1-803-777-6781.
E-mail addresses: Adams@mail.chem.sc.edu, jomc@mail.chem.sc.edu (R.D. Adams).

0022-328X/$ - see front matter © 2004 Elsevier B.V. All rights reserved.
doi:10.1016/j.jorganchem.2003.12.028

2. Results and discussion

The new diirondimanganese compound [CpFeMn(CO)$_5$(μ_3-S$_2$)]$_2$, **2** was obtained in 62% yield from the reaction of thiirane with CpFeMn(CO)$_7$ when activated by Me$_3$NO at 25 °C, Eq. (1). The infrared spectrum of **2** shows four absorptions consistent with terminal carbonyl ligands. The ^{1}H NMR spectrum exhibits a single resonance for the Cp ligand at $\delta = 4.01$ ppm. The molecular structure of **2** was established by a single crystal X-ray diffraction analysis, and an ORTEP diagram of its molecular structure is shown in Fig. 1. Selected bond distances and angles for **2** are listed in Table 1.

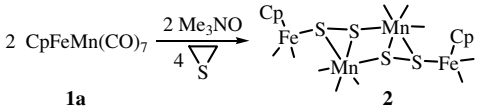

(1)

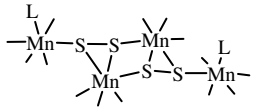

5, L = AsMe$_2$Ph
6, L = PMe$_2$Ph

The structure of **2** consists of an open tetranuclear metal cluster containing two manganese and two iron atoms with two triply bridging disulfido ligands. In the solid state, compound **2** lies on an inversion center that is located in the center of the central Mn$_2$S$_2$ group of atoms. The manganese atoms are bridged by two of the sulfur atoms of the disulfido ligands, S(2) and S(2′), and the central Mn$_2$S$_2$ group is planar. Compound **2** is structurally similar to the dimeric compounds Mn$_4$(CO)$_{14}$L$_2$(μ_3-S$_2$)$_2$ (**5**, L = AsMe$_2$Ph and **6**, L = PMe$_2$Ph) [7]. Compound **5** was obtained by the addition of AsMe$_2$Ph to Mn$_2$(CO)$_7$(μ-S$_2$) [7]. The Mn(1)–S(2) and Mn(1)–S(2′) bond distances in **2**, 2.3897(6) and 2.4069(6) Å, respectively, are very similar to the corresponding distances in **5**, 2.4100(13), 2.3801(12) Å, and **6**, 2.3805(7), 2.4142(7) Å. The second disulfido sulfur atom S(1) is bonded to one manganese atom, the iron atom of the pendant CpFe(CO)$_2$ group and the second sulfur atom S(2). The S–S distance in **2**, S(1)–S(2) = 2.0740(8) Å, is not significantly different from the S–S distances in **5**, 2.0701(15) Å and **6**, 2.0732(8) Å. There are no metal–metal bonds in the complex. The bridging disulfido ligands serve as 6 electron donors and all metal atoms achieve 18 electron configurations. We could not find any evidence for a heterodinuclear (ironmanganesedisulfido) form of this complex, e.g., CpFeMn(CO)$_4$(μ-S$_2$), that would be the iron analogue of Cp MoMn(CO)$_5$(μ-S$_2$) which we have previously reported [8].

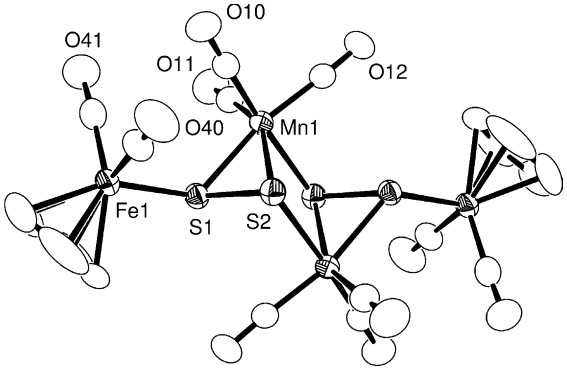

Fig. 1. An ORTEP diagram of [CpFeMn(CO)$_5$(μ_3-S$_2$)]$_2$, **2** showing 50% probability thermal ellipsoids.

Table 1
Selected intramolecular distances and angles for compounds **2** and **3**

Atom	Atom	Distance (Å)	
2			
Mn(1)	S(1)	2.3193(6)	
Mn(1)	S(2)	2.3897(6)	
Mn(1)	S(2′)	2.4069(6)	
Fe(1)	S(1)	2.2664(6)	
S(1)	S(2)	2.0740(8)	
Mn(1)	Mn(1′)	3.6773(7)	
3			
Mn(1)	S(1)	2.4025(11)	
Mn(1)	S(2)	2.3207(11)	
Mn(1)	S(1′)	2.3621(11)	
Fe(1)	S(2)	2.2605(10)	
S(1)	S(2′)	2.0685(14)	
Mn(1)	Mn(1′)	3.5564(11)	
Atom	Atom	Atom	Angle (°)
2			
S(1)	Mn(1)	S(2)	52.24(2)
S(1)	Mn(1)	S(2′)	86.48(2)
S(2)	Mn(1)	S(2′)	79.89(2)
S(2)	S(1)	Fe(1)	114.65(3)
S(2)	S(1)	Mn(1)	65.63(2)
Fe(1)	S(1)	Mn(1)	125.06(3)
S(1)	S(2)	Mn(1)	62.14(2)
S(1)	S(2)	Mn(1′)	97.68(3)
Mn(1)	S(2)	Mn(1′)	100.11(2)
3			
S(2)	Mn(1)	S(1′)	52.42(4)
S(2)	Mn(1)	S(1)	91.35(4)
S(1′)	Mn(1)	S(1)	82.48(4)
S(2′)	S(1)	Mn(1′)	62.76(4)
S(2′)	S(1)	Mn(1)	108.96(5)
Mn(1′)	S(1)	Mn(1)	96.56(4)
S(1′)	S(2)	Fe(1)	108.99(5)
S(1′)	S(2)	Mn(1)	64.82(4)
Fe(1)	S(2)	Mn(1)	124.45(4)

Estimated standard deviations in the least significant figure are given in parentheses.

Atoms with (′) are related to the corresponding unprimed atoms by a center of symmetry operation.

The Cp* analogue of **2** [CpFeMn(CO)$_5$(μ_3-S$_2$)]$_2$, **3**, was obtained by performing the reaction as described

above with substitution of $Cp^*FeMn(CO)_7$ for $CpFeMn(CO)_7$. The molecular structure of **3** was also established crystallographically. An ORTEP diagram of its molecular structure is shown in Fig. 2. Selected bond distances and angles for **3** are listed in Table 1. Like compound **2**, compound **3** is a dimer of the unit $CpFeMn(CO)_5(\mu_3\text{-}S_2)$ and contains two iron atoms, two manganese atoms and two bridging disulfido ligands. However, it does have a different structural conformation for the bridging sulfido ligands. In the solid state, this molecule contains $\boldsymbol{C_2}$ rotational symmetry. Two of the sulfur atoms bridge the two central manganese atoms as in **2**, with similar Mn–S bond distances, Mn(1)–S(1) = 2.4025(11) Å and Mn(1)–S(1′) = 2.3621(11) Å. The second sulfur atom of each disulfido ligand contains a pendant $Cp^*Fe(CO)_2$, but unlike **2** where the two iron groups lay on opposite sides of the central Mn_2S_2 plane in a chair-like conformation, in **3** both iron groups lie on the same side of the central Mn_2S_2 group in a boat-like conformation, and the Mn_2S_2 group is not planar. The dihedral angle between the two MnS_2 planes is 10.59(6)°.

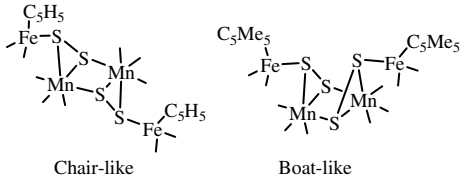

The S–S distance in **3**, S(1)–S(2′) = 2.0685(14) Å, is slightly shorter than that observed in **2**.

When compound **2** was heated to 40 °C, the new complex $Cp_3Fe_3Mn_3(CO)_{15}(\mu_3\text{-}S_2)(\mu_4\text{-}S_2)_2$, **4** was obtained in 22% yield. Compound **4** was also characterized crystallographically, and an ORTEP diagram of its molecular structure is shown in Fig. 3. Selected bond distances and angles for **4** are listed in Table 2. The molecule contains three manganese tricarbonyl groups that are linked by three bridging disulfido ligands. Each disulfido ligand contains one pendant $CpFe(CO)_2$ group. Two of the disulfido ligands, S(1)–S(2) and S(3)–S(4), are quadruply bridging ligands. The third, S(5)–S(6), is a triply bridging ligand. S(3)–S(4) serves as an 8 electron donor to the metal atoms, S(1)–S(2) serves as a 6 electron donor and S(5)–S(6) serves as a 4 electron donor. All metal atoms achieve the 18 electron configuration, and there are no metal–metal bonds in the complex. The S–S bond distances for the quadruply bridging sulfido ligands, S(1)–S(2) = 2.0929(12) Å and S(3)–S(4) = 2.0951(12) Å, are slightly longer than that of the triply bridging ligand, S(5)–S(6) = 2.0835(13) Å.

There is no loss of ligands in the formation of **4** from **2**, Eq. (2). Compound **4** can be viewed as a trimer of the unobserved monomer "$CpFeMn(CO)_5(\mu\text{-}S_2)$", and it seems likely that a splitting of the dimer to produce a transient form of the monomer may have been involved in the formation of **4**, but we have no evidence for the independent existence of the monomeric form at this time. The reaction is a simple aggregation process and appears not to be reversible.

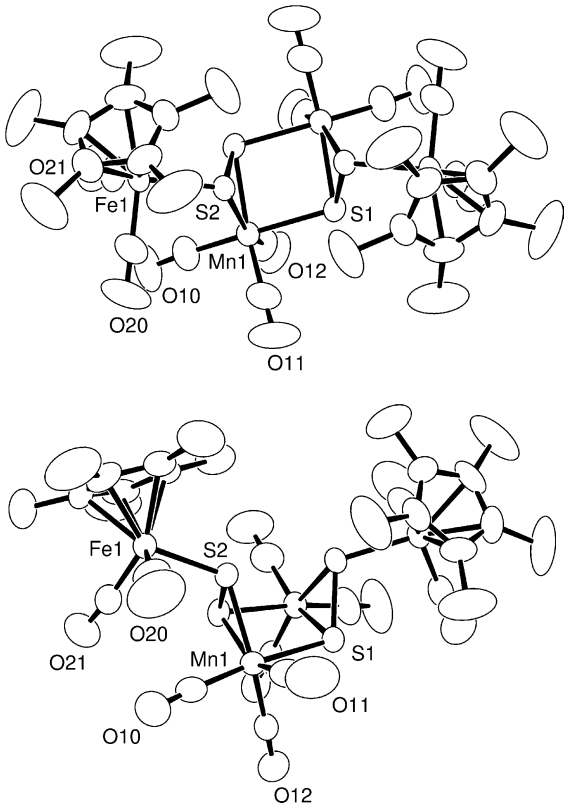

Fig. 2. An ORTEP diagram of $[Cp^*FeMn(CO)_5(\mu_3\text{-}S_2)]_2$, **3** showing 50% probability thermal ellipsoids.

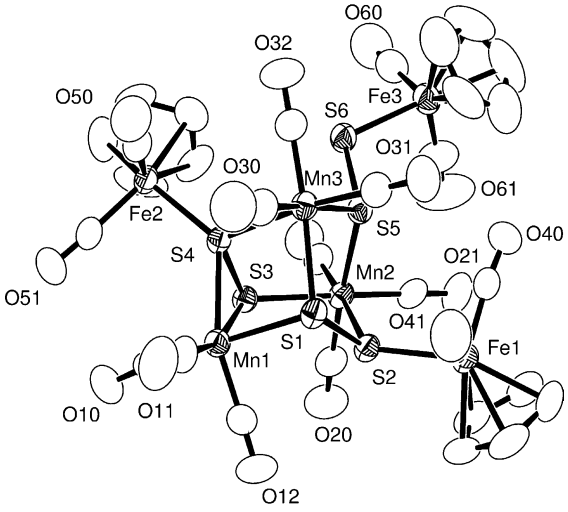

Fig. 3. An ORTEP diagram of $Cp_3Fe_3Mn_3(CO)_{15}(\mu_3\text{-}S_2)(\mu_4\text{-}S_2)_2$, **4** showing 50% probability thermal ellipsoids.

Table 2
Selected intramolecular distances and angles for compound **4**

Atom	Atom	Distance (Å)	
Mn(1)	S(3)	2.3415(10)	
Mn(1)	S(4)	2.3616(10)	
Mn(1)	S(1)	2.3802(10)	
Mn(2)	S(3)	2.3365(10)	
Mn(2)	S(2)	2.3636(10)	
Mn(2)	S(5)	2.3774(10)	
Mn(3)	S(4)	2.3637(10)	
Mn(3)	S(1)	2.3653(10)	
Mn(3)	S(5)	2.3909(10)	
Fe(1)	S(2)	2.2948(10)	
Fe(2)	S(4)	2.2725(9)	
Fe(3)	S(6)	2.2838(11)	
S(1)	S(2)	2.0929(12)	
S(3)	S(4)	2.0951(12)	
S(5)	S(6)	2.0835(13)	
Atom	Atom	Atom	Angle (°)
S(3)	Mn(1)	S(4)	52.90(3)
S(3)	Mn(1)	S(1)	88.50(3)
S(4)	Mn(1)	S(1)	78.53(3)
S(3)	Mn(2)	S(2)	89.26(3)
S(3)	Mn(2)	S(5)	93.33(3)
S(2)	Mn(2)	S(5)	85.68(3)
S(4)	Mn(3)	S(1)	78.79(3)
S(4)	Mn(3)	S(5)	90.89(3)
S(1)	Mn(3)	S(5)	90.86(3)
S(2)	S(1)	Mn(3)	112.05(4)
S(2)	S(1)	Mn(1)	99.67(4)
Mn(3)	S(1)	Mn(1)	100.11(3)
S(1)	S(2)	Fe(1)	110.27(5)
S(1)	S(2)	Mn(2)	105.96(4)
Fe(1)	S(2)	Mn(2)	122.20(4)
S(4)	S(3)	Mn(2)	114.32(5)
S(4)	S(3)	Mn(1)	64.04(3)
Mn(2)	S(3)	Mn(1)	118.06(4)
S(3)	S(4)	Fe(2)	113.23(4)
S(3)	S(4)	Mn(1)	63.06(3)
Fe(2)	S(4)	Mn(1)	130.84(4)
S(3)	S(4)	Mn(3)	110.17(4)
Fe(2)	S(4)	Mn(3)	123.27(4)
Mn(1)	S(4)	Mn(3)	100.70(3)
S(6)	S(5)	Mn(2)	112.67(5)
S(6)	S(5)	Mn(3)	109.92(5)
Mn(2)	S(5)	Mn(3)	111.43(4)
S(5)	S(6)	Mn(3)	108.83(5)

Estimated standard deviations in the least significant figure are given in parentheses.

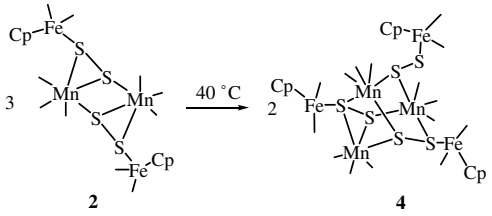

(2)

Indeed when **4** is heated, it goes on to form other compounds that may be of still higher nuclearity species, but these have so far defied characterization.

The ^{1}H NMR spectrum of **4** exhibits three singlets of equal intensity at $\delta = 4.56$, 4.43 and 4.22 ppm at 25 °C indicating that all three cyclopentadienyl groups are inequivalent. This is consistent with the structure observed in the solid state. Interestingly, however compound **4** does exhibit some unexpected molecular dynamics as shown by its variable temperature ^{1}H NMR spectra, see Fig. 4. In particular, the two resonances at 4.43 and 4.22 ppm undergo reversible line broadening as the temperature is raised above room temperature. These two resonances merge at about 70 °C and the averaged resonance continues to sharpen as shown in the 75 °C spectrum (top of Fig. 4), but at this temperature the compound begins to decompose rapidly as indicated by the new resonances marked with * in the spectrum at this temperature. Simulated line shaped calculations of the exchange broadened spectra have provided exchange rates that have in turn provided activation parameters for the process: $\Delta H^{\ddagger} = 13.7(4)$ kcal/mol, $\Delta S^{\ddagger} = -7(1)$ cal/mol K, $\Delta G^{\ddagger}$ (at 343 K) = 16.1(7) kcal/mol.

A proposed mechanism to explain these spectral changes is shown in Fig. 5. The rearrangement proceeds as follows: (1) The Mn(1)–S(4) bond breaks to form the intermediate **A**. Provided that the sulfur atom S(5) is able to invert its configuration rapidly on the NMR time scale, this renders the two iron cyclopentadienyl groups Fe(1)Cp(1) and Fe(2)Cp(2) equivalent by virtue of its C_2 symmetry. It has been shown in previous studies that the sulfur atom of bridging thiolato ligands do invert their configurations rapidly on the NMR timescale at moderate temperatures [10]. (2) From **A** either of the sulfur atoms S(4) or S(2) can form a bond to Mn(1). If the bond to S(2) is formed, then the interchange of Fe(1)Cp(1) and Fe(2)Cp(2) groups is completed.

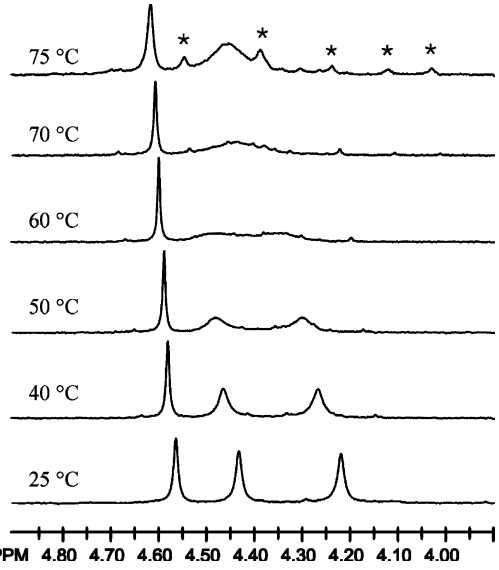

Fig. 4. ^{1}H NMR spectra of compound **4** at various temperatures in toluene(d_8) solvent. Resonances marked with * are unidentified decomposition products that begin to form at the higher temperatures.

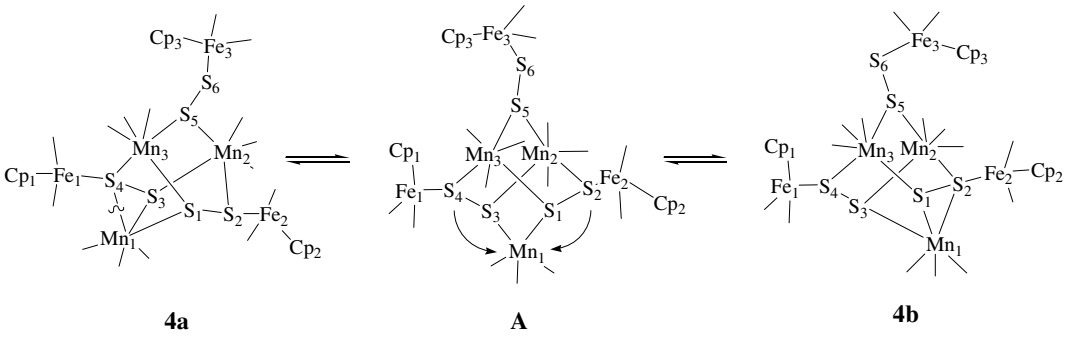

Fig. 5. A mechanism for the dynamical interchange of two of the three $CpFe(CO)_2$ groups of compound **4**.

Alternatively, an equivalent exchange could be effected by a nucleophilic displacement of S(4) by S(2) at atom Mn(1). This would eliminate the need for the intermediate **A** in which the atom Mn(1) has only a 16 electron configuration. There may be still other mechanisms for effecting the interchange of two of the three $CpFe(CO)_2$ groups in **4** without involving the third one.

As we have already shown [7], these studies further demonstrate that stable high nuclearity metal complexes containing bridging disulfide ligands can be formed as oligomers of lower nuclearity species, and they can be readily isolated and structurally characterized even if the monomer itself is not isolable. This is facilitated by the ability of the disulfido ligand to coordinate both of its sulfur atoms and serve as a multi-electron donor to the metal atoms.

3. Experimental

General data. All reactions were performed under a nitrogen atmosphere by using Schlenk techniques. Reagent grade solvents were dried by the standard procedures and were freshly distilled prior to use. Infrared spectra were recorded on a Thermo-Nicolet Avatar FTIR spectrophotometer. ^1H NMR spectra were recorded on a Mercury 300 spectrometer operating at 300 MHz. Variable temperature NMR spectra were recorded on a Varian Inova 500 spectrometer operating at 500 MHz. Elemental analyses were performed by Desert Analytics (Tucson, AZ). $Me_3NO \cdot 2H_2O$ was purchased from Aldrich Co. $CpFeMn(CO)_7$, **1a** was prepared according to the published procedures [11]. $Cp^*FeMn(CO)_7$, **1b** was prepared similarly. Unless stated otherwise, all product separations were performed by TLC in air on Analtech 0.25 and 0.5 mm silica gel 60 Å F_{254} glass plates.

Reaction of activated $CpFeMn(CO)_7$ with thiirane. A sample of $CpFeMn(CO)_7$ (75.0 mg, 0.202 mmol) was dissolved in 20 mL MeCN in a 50 mL three-neck round-bottom flask equipped with a stir bar, gas inlet and gas outlet. To this solution was added 23.0 mg (0.202 mmol) of $Me_3NO \cdot 2H_2O$ and the resulting solution was allowed to stir at room temperature for 1 h in the absence of light. The solvent was removed in vacuo and the residue was dissolved in 30 mL hexane and 10 mL CH_2Cl_2. Then three equivalents of thiirane were added via syringe and the solution was allowed to stir for 24 h in the dark. The volatiles were removed in vacuo and the residue was separated by column chromatography over silica-gel by using hexane/methylene chloride (1/2, v/v) solvent mixture as eluent. This provided in order of elution: 6.5 mg of unreacted **1** and 47.7 mg (62%) of dark-red $[CpFeMn(CO)_5(\mu_3\text{-}S_2)]_2$, **2**. Spectral data for **2**: IR ν_{CO} (cm^{-1} in CH_2Cl_2) 2047 (s), 2008 (vs), 1991 (s), 1911 (s). ^1H NMR (δ in C_6D_6) 4.007 (s, 10H). Anal. Calc. for $[CpFeMn(CO)_5(\mu_3\text{-}S_2)]_2$: C, 31.60; H, 1.33. Found C, 31.32; H, 1.20%.

Reaction of activated $Cp^*FeMn(CO)_7$ with thiirane. A sample of $Cp^*FeMn(CO)_7$ (44.0 mg, 0.10 mmol) was dissolved in 5 mL MeCN in a 25 mL three-neck round-bottom flask equipped with a stir bar, gas inlet and gas outlet. To this solution was added 17.0 mg (0.15 mmol) of $Me_3NO \cdot 2H_2O$ and the resulting solution was allowed to stir at room temperature for 1 h in the absence of light. The solvent was removed in vacuo and the residue was dissolved in 15 mL hexane and 1 mL CH_2Cl_2. Added two equivalents (15 μL) of thiirane via syringe and allowed to stir at room temperature overnight. Removed volatiles in vacuo. The residues were separated by column chromatography over alumina by using hexane/CH_2Cl_2 (1/9, v/v) solvent mixture as eluant. 8.8 mg (20 %) of dark-red $[Cp^*FeMn(CO)_5(\mu_3\text{-}S_2)]_2$, **3** was obtained. Spectral data for **3**: IR ν_{CO} (cm^{-1} in CH_2Cl_2) 2034 (m), 2026 (s), 1990 (vs), 1909 (br, s). ^1H NMR (δ in CD_2Cl_2) 1.919 (s, 15H). Anal. Calc. for $[Cp^*FeMn(CO)_5(\mu_3\text{-}S_2)]_2$: C, 40.02; H, 3.36. Found C, 39.54; H, 3.17%.

*Thermolysis of **2**.* A sample of **2** (17.3 mg, 0.0228 mmol) was dissolved in 15 mL of deoxygenated methylene chloride in a 25 mL three-neck round-bottom flask equipped with a stir bar, gas inlet and gas outlet. The resulting solution was heated to reflux for 11 h in the absence of light. The solvent was removed in vacuo and

the residues were separated by TLC by using hexane/CH_2Cl_2 (1/2, v/v) solvent mixture as eluant. This yielded 3.8 mg (22%) of brown $Cp_3Fe_3Mn_3(CO)_{15}(\mu_3\text{-}S_2)(\mu_4\text{-}S_2)_2$, **4**. Spectral data for **4**: IR ν_{CO} (cm^{-1} in CH_2Cl_2) 2058 (m), 2046 (m), 2033 (m), 2016 (s), 2000 (vs), 1930 (br, s). ^1H NMR (δ in touene-d_8) 4.564 (s, 5H), 4.432 (s, 5H), 4.218 (s, 5H). Anal. Calc. for $Cp_3Fe_3Mn_3(CO)_{15}(\mu_3\text{-}S_2)(\mu_4\text{-}S_2)_2$: C, 31.60; H, 1.33. Found C, 31.75; H, 1.69%.

NMR calculations. Line-shape analyses were performed on a Gateway PC by using the program EXCHANGE written by R.E.D. McClung of the Department of Chemistry, University of Alberta, Edmonton, Alberta, Canada. For compound **4** exchange rates were determined at six different temperatures in the temperature range 25–75 °C. The activation parameters were determined from a best-fit Eyring plot using the program Microsoft Excel: $\Delta H^{\ddagger} = 13.7(4)$ kcal/mol, $\Delta S^{\ddagger} = -7(1)$ cal/mol K.

Crystallographic analyses. Single crystals of **2** (red) and **4** (dark-red) were grown by slow evaporation of the solvent from a benzene/octane solution of the complex at 4 °C. Single crystals of **3** (dark-red) suitable for diffraction analysis were grown by slow evaporation of solvent from a solution of the compound in a hexane/methylene chloride solvent mixture at −17 °C. All crystals used for X-ray data collections were glued onto the end of a thin glass fiber. X-ray intensity data for each structural analysis was collected on a Bruker SMART APEX CCD-based diffractometer using Mo Kα radiation ($\lambda = 0.71073$ Å). The unit cells were determined on the basis of reflections obtained from sets of three orthogonal scans. Crystal data, data collection parameters, and results of the analyses are listed in Table 3. The raw intensity data frames were integrated with SAINT+ program [12], which also applied corrections for Lorentz and polarization effects. Final unit cell parameters are based on the least-squares refinement of all reflections with $I > 5(\sigma)I$ from the data sets. For each analysis an empirical absorption correction based on the multiple measurement of equivalent reflections was applied by using SADABS. Compounds **2** and **3** crystallized in the monoclinic system. The space group $P2_1/c$ was confirmed by the systematic absences in the intensity data for compound **2**. For compound **3** the space groups $C2/c$ and Cc were indicated by the systematic absences in the intensity data. The former space group was assumed and confirmed by the solution and refinement of the structure. Compound **4** crystallized in the triclinic crystal system. The space group $P\bar{1}$ was assumed and confirmed by the successful solution and refinement of the structure. All structures were solved by a combination of direct methods and difference Fourier syntheses, and were refined by full-matrix least-squares on F^2 by using SHELXTL program library [13] and neutral atom scattering factors. For each structure, all non-hydrogen atoms were refined with anisotropic displacement parameters. The positions of the hydrogen

Table 3
Crystallographic data for compounds **2**–**4**

	2	3	4
Empirical formula	$FeMnS_2O_5C_{10}H_5 \cdot 1/2C_6H_6$	$Fe_2Mn_2S_4O_{10}C_{30}H_{30}$	$Fe_3Mn_3S_6O_{15}C_{30}H_{15} \cdot C_6H_6$
Formula weight	419.10	900.36	1218.26
Crystal system	Monoclinic	Monoclinic	Triclinic
Lattice parameters			
a (Å)	9.0128(6)	20.7088(9)	11.7750(5)
b (Å)	16.3311(11)	10.2520(5)	14.0705(6)
c (Å)	11.1087(7)	17.7186(8)	14.1440(6)
α (°)	90	90	92.193(1)
β (°)	110.154(1)	91.841(1)	108.317(1)
γ (°)	90	90	94.185(1)
V (Å^3)	1534.96(17)	3759.8(3)	2214.07(16)
Space group	$P2_1/c$	$C2/c$	$P\bar{1}$
Z value	4	4	2
ρ_{calc} (g/cm^3)	1.814	1.591	1.827
μ(Mo Kα) (mm^{-1})	2.056	1.685	2.135
Temperature (K)	296	296	296
$2\Theta_{max}$ (°)	52.04	52.04	52.00
No. obs. ($I > 2\sigma(I)$)	2710	2796	7366
No. parameters	119	222	568
Goodness of fit	1.072	1.043	1.115
Max. shift in final cycle	0.001	0.001	0.001
Residuals*: R_1; wR_2	0.0277; 0.0670	0.0482; 0.1086	0.0426; 0.0970
Transmission coeff., max/min	1.0/0.74	1.0/0.81	1.0/0.76
Largest peak in final diff. four (e$^-$/Å^3)	0.346	0.438	0.468

* $R_1 = \sum(||F_{obs}| - |F_{calc}||)/\sum|F_{obs}|$. $wR_2 = \{\sum[w(F^2_{obs} - F^2_{calc})^2]/\sum[w(F^2_{obs})^2]\}^{1/2}$; $w = 1/\sigma^2(F^2_{obs})$. GoF $= [\sum_{hkl}(w(|F^2_{obs}| - |F^2_{calc}|))^2/(n_{data} - n_{vari})]^{1/2}$.

atoms were calculated by assuming idealized geometries. These were included as riding atoms in the final cycles of refinement in each structural analysis.

4. Supplementary material

CIF tables for the structural analyses of compounds **2**–**4** have been deposited with the Cambridge Crystallographic Data Center. The deposit numbers are CCDC 219650–219652.

Acknowledgements

This research was supported by a grant from the National Science Foundation, Grant No. CHE-9909017.

References

[1] (a) H. Ogino, S. Inomata, H. Tobita, Chem. Rev. 98 (1998) 2093;
(b) K.H. Whitmire, J. Coord. Chem. 17 (1988) 95.
[2] (a) M. Hidai, S. Kuwata, Y. Mizobe, Account Chem. Res. 33 (2000) 46;
(b) S.-W. Audi Fong, T.S.A. Hor, J. Chem. Soc., Dalton Trans. (1999) 639;
(c) T. Shibihara, Coord. Chem. Rev. 123 (1993) 73;
(d) R.D. Adams, M. Tasi, J. Cluster Sci. 1 (1990) 249;
(e) R.D. Adams, Polyhedron 4 (1985) 2003.
[3] (a) A. Müller, W. Jaegermann, J. Enemark, Coord. Chem. Rev. 46 (1982) 245;
(b) K. Matsumoto, T. Koyama, T. Furuhashi, ACS Sym. Ser. 653 (1996) 251.
[4] (a) A. Müller, E. Diemann, Adv. Inorg. Chem. 31 (1987) 89;
(b) J. Amaraskera, T.B. Rauchfuss, S.R. Wilson, Inorg. Chem. 26 (1987) 3328;
(c) K. Yoshioka, H. Kikuchi, J. Mizutani, K. Matsumoto, Inorg. Chem. 40 (2001) 2234.
[5] (a) J. Wachter, Angew. Chem. Int. Ed. Engl. 28 (1989) 1613;
(b) R.B. King, T.E. Bitterwolf, Coord. Chem. Rev. 206–207 (2000) 563;
(c) K.H. Whitmire, in: G. Wilkinson, F.G.A. Stone, E. Abel (Eds.), Comprehensive Organometallic Chemistry II, vol. 7, Pergamon Press, New York, 1995, p. 62 (Chapter 1, section 1.11.2.2) and references therein.
[6] R.D. Adams, O.S. Kwon, M.D. Smith, Inorg. Chem. 40 (2001) 5322.
[7] R.D. Adams, O.S. Kwon, M.D. Smith, Inorg. Chem. 41 (2002) 6281.
[8] R.D. Adams, B. Captain, O.S. Kwon, S. Miao, Inorg. Chem. 42 (2003) 5322.
[9] (a) R.D. Adams, O.S. Kwon, M.D. Smith, Inorg. Chem. 41 (2002) 5525;
(b) R.D. Adams, O.S. Kwon, M.D. Smith, Organometallics 21 (2002) 1960;
(c) R.D. Adams, O.S. Kwon, M.D. Smith, Inorg. Chem. 41 (2002) 1658.
[10] R.D. Adams, D.A. Katahira, L.-W. Yang, Organometallics 1 (1982) 235.
[11] P. Johnston, G.J. Hutchings, L. Denner, J.C.A. Boeyens, N.J. Coville, Organometallics 6 (1987) 1292.
[12] SAINT+ Version 6.02a. Bruker Analytical X-ray System, Inc., Madison, WI, USA, 1998.
[13] G.M. Sheldrick, SHELXTL Version 5.1, Bruker Analytical X-ray Systems, Inc., Madison, WI, USA, 1997.